Microporous and Mesoporous Materials 118 (2009) 354–360

Contents lists available at ScienceDirect

Microporous and Mesoporous Materials

journal homepage: www.elsevier.com/locate/micromeso

Vanadia supported on H_2O_2-detemplated mesoporous SBA-15 as new effective catalysts for the oxidative dehydrogenation of propane

Jie Xu, Miao Chen, Yong-Mei Liu, Yong Cao *, He-Yong He, Kang-Nian Fan *

Department of Chemistry and Shanghai Key Laboratory of Molecular Catalysis and Innovative Materials, Fudan University, Shanghai 200433, PR China

ARTICLE INFO

Article history:
Received 11 July 2008
Received in revised form 3 September 2008
Accepted 4 September 2008
Available online 11 September 2008

Keywords:
Vanadia
SBA-15
Mesoporous materials
Oxidative dehydrogenation (ODH) of propane
Propylene
H_2O_2

ABSTRACT

Mesoporous SBA-15(H_2O_2) material synthesized via a controlled H_2O_2-based detemplation at mild conditions has been employed as new type of support to load vanadia. The ordered mesostructure of the SBA-15 host is retained as indicated by XRD and nitrogen adsorption measurements, and the surface areas of the V-SBA-15(H_2O_2) materials are in the range of 464–667 $m^2 g^{-1}$ comparable to 772 $m^2 g^{-1}$ for the parent SBA-15(H_2O_2) material. The characterization results also indicate the presence of a high abundance of surface silanol groups inside the silica pores, which can allow controlled vanadia loading up to 4.5 wt% or *V* coverage up to 1.01 V nm^{-2}. In contrast to conventional calcination-derived SBA-15(C) sample the high population of the surface hydroxyl groups as well as high structural stability of the SBA-15(H_2O_2) material allowed a very good dispersion of the vanadia on its surface leading to high productivities of propylene during the oxidative dehydrogenation of propane.

1. Introduction

As a major building block of the modern petrochemical industry, propylene is heavily used for the production of diverse products ranging from solvents to plastics [1,2]. Currently, propylene is mainly produced by steam cracking or a direct dehydrogenation (DH) of various hydrocarbon feedstocks at high temperatures, where intensive energy consumption and coking present serious problems [1,3–5] With the constantly growing propylene market and rapidly rising fuel costs, the catalytic oxidative dehydrogenation (ODH) of propane has attracted tremendous recent attention as an energy-saving and cost-efficient alternative for the production of propylene [4–14]. This process is thermodynamically favored at much lower temperatures and usually does not lead to the formation of coke and smaller hydrocarbons [6,8,9]. However, this selective oxidation is particularly challenging, given the high reactivity of propylene toward further oxidation or combustion under reaction conditions [3–10].

SiO_2-supported vanadia catalysts (including V-containing microporous and mesoporous materials) have been reported to be active and selective for the ODH of propane [15–22]. An important dependence between vanadium content and catalytic performance has been observed [17–19], in a way that low V-loading catalysts present the highest selectivity to propylene. Unfortunately, the productivities to propylene in these materials are low due to the presence of few active sites in the selective catalysts [18]. For this reason, and in order to obtain high selectivity to propylene while improving the productivity, some high surface mesoporous siliceous materials have been proposed as supports as MCM-41, MCM-48 or SBA-15 [18–21]. These materials are capable to disperse higher amounts of vanadium without losing the selectivity to propylene. The main drawback is that these catalysts do not always maintain its structure if high vanadium contents (>5 wt%) are incorporated to the catalyst [20,21].

In continued search for more effective technologies for propylene production, there is a definite need for new improved vanadia-based catalysts that can allow more efficient ODH of propane [20]. Very recently, we have reported that the use of mesoporous MCF silica as a support can allow the generation of a highly efficient V–MCF catalyst exhibiting high propylene productivities in the ODH of propane [22]. The excellent performance of V–MCF has been attributed to the presence of a high abundance of silanol groups of the MCF material that can allow the favorable creation of a higher surface concentration of isolated VO_x species in the V–MCF system. According to this result, one might anticipate that using high surface area mesoporous siliceous materials featured with higher amount of surface hydroxyl groups as a support may allow the devise of improved V-containing materials with higher active site densities for the ODH of propane.

* Corresponding authors. Tel.: +86 21 55665287; fax: +86 21 65642978.
E-mail addresses: yongcao@fudan.edu.cn (Y. Cao), knfan@fudan.edu.cn (K.-N. Fan).

1387-1811/$ - see front matter © 2008 Elsevier Inc. All rights reserved.
doi:10.1016/j.micromeso.2008.09.007

In the present work, we report the development of new efficient SBA-15 supported vanadia system exhibiting enhanced activity and productivity for the ODH of propane. H_2O_2-mediated oxidation catalyzed by traces of Fe^{3+}, previously established to be an effective versatile procedure known as "Fenton-type process" for treating industrial organic pollutants [23], have shown to be particularly useful for the synthesis of surfactant-free mesoporous SBA-15 silica featured with a high abundance of surface silanol groups. Our results have shown that the alcoholic impregnation of vanadium oxide species onto the inner walls of H_2O_2-detemplated SBA-15 can allow the favorable creation of a high population of isolated surface VO_x sites with V-loading up to 4.5 wt%, which makes the catalysts highly active and selective for the reaction.

2. Experimental

2.1. Catalyst preparation

Pure siliceous SBA-15 samples were synthesized following the technique reported by Zhao et al. [24] In a typical synthesis, 2.0 g of Pluronic P123 ($EO_{20}PO_{70}$–EO_{20}, Aldrich) was dissolved in the mixture of 15 ml of water and 60 ml of 2 mol L^{-1} HCl with stirring, and then 4.25 g of tetraethyl orthosilicate (TEOS, Aldrich) was added. The resulting reaction mixture was stirred at 40 °C for 5 h, and then hydrothermally treated at 95 °C for 72 h under static condition in a Teflon-lined stainless steel autoclave. The resulting solid products were filtered, washed with distilled water and dried in the air at 80 °C overnight to obtain as-synthesized SBA-15 (designated as SBA-15(A)).

SBA-15(A) was treated twice with 30 wt% H_2O_2 solution (liquid-to-solid ratio of 50 mL g^{-1}) in a flask at 80 °C for 20 h under continuous stirring, then filtered and dried at ambient conditions to obtain the resulting detemplated material of SBA-15(H_2O_2). Prior to above treatment, a concentration of ca. 200 ppm of Fe^{3+} was introduced into SBA-15(A) by dispersing 6.0 g of SBA-15(A) into a 10 mL solution containing 1.2 mg of $FeCl_3 \cdot 6H_2O$, which can initiate the propagation of the $OH^{\bullet}$ radicals, subsequent oxidizing and removing the template via Fenton-based processing [25]. A reference sample denoted as SBA-15(C) was obtained by calcining SBA-15(A) in a muffle oven at 600 °C for 4 h.

Vanadium loaded SBA-15 catalysts were prepared through a wet impregnation method. SBA-15(H_2O_2) or SBA-15(C) was dispersed in a methanol solution of NH_4VO_3 at 60 °C. After evaporating the solvent at 110 °C, the solid samples were calcined at 600 °C in static air for 2 h. Thus the prepared catalysts were designated as *n*V-SBA-15(H_2O_2) and *n*V-SBA-15(C) (where *n* is the V-content in wt% of V-atoms), respectively.

2.2. Catalyst characterization

The vanadium contents in all catalysts were measured by ICP-AES after solubilization of the samples in HF/HCl solutions. Nitrogen adsorption and desorption at 196 °C were measured using a Micromeritics TriStar 3000 after the samples were degassed (1.33×10^{-2} Pa) at 300 °C overnight. The specific surface area was calculated using the BET method, and pore size distribution was determined by the BJH method.

Diffuse reflectance infrared Fourier transform (DRIFT) characterization of the catalysts was performed using a Bruker Vector 22 instrument equipped with a DTGS detector and a KBr beam splitter [22]. The samples were placed in a sample cup inside a Harrick diffuse reflectance cell equipped with ZnSe windows and a thermocouple mount that allowed direct measurement of the sample temperature. All spectra were collected in dry air atmosphere at 200 °C.

Small angle XRD patterns were collected using a Germany Bruker D8Advance X-ray diffractometer equipped with a graphite monochromator, operating at 40 kV and 40 mA and employing nickel-filtered Cu-Kα radiation. Thermo gravimetric analysis (TGA) was performed using a Perkin-Elmer TGA 7 analyzer with a heating rate of 20 °C min^{-1} under an air flow of 30 mL min^{-1}.

In situ laser Raman spectra were obtained using a confocal microprobe Jobin Yvon Lab. Ram Infinity Raman system equipped with both visible and UV excitation lines. The visible Raman measurements were carried out using internal Ar^+ excitation at 514.5 nm with a power of 10 mW. The sample was loaded in an *in situ* cell and was pretreated in dry airflow at 450 °C for 1 h for dehydration. All spectra were recorded at 200 °C in N_2 gas flow with a resolution of 4 cm^{-1}.

Temperature-programmed reduction (TPR) profiles were obtained on a homemade apparatus as described elsewhere [19]. Approximate 20 mg of a freshly calcined catalyst was placed on top of glass wool in a quartz reactor. TPR experiments were carried out in 5% H_2/Ar flowing at 40 mL min^{-1}, with a ramping rate of 10 °C min^{-1} to a final temperature of 700 °C. The H_2 consumption was monitored using a TCD detector.

2.3. Catalytic activity measurements

The catalytic properties were investigated in a fixed-bed quartz tubular flow reactor (6 mm i.d. 400 mm length) equipped with several gas flow lines with mass flow controllers to supply the feed, consisting of a mixture of propane/oxygen/nitrogen with a molar ratio of 1/1/4 (unless otherwise specified, the total flow rate fixed at 18 mL min^{-1}). The temperature in the middle of the catalytic bed was measured with a coaxial thermocouple. Catalyst samples (W_{cat} = 25 mg, 60–80 mesh) were introduced into the reactor and diluted with 300 mg of quartz powder (40–60 mesh) to maintain a constant volume in the catalyst bed. The product was analyzed by on-line chromatography.

3. Results and discussion

3.1. Catalyst characterization

The effectiveness of the detemplation by H_2O_2-mediated oxidation is demonstrated by TG analysis (Fig. 1A). The TG profile of SBA-15(A) shows two major weight losses around <150, 150–850 °C. The first is due to physisorbed water, while the second comes from the template [27]. The weight loss for SBA-15(A) at temperature between 150 and 850 °C is ca. 41.6 wt%, which is similar to the content of the ionic surfactant template in typical MCM-41 and MCM-48 silicas. The TGA profile of SBA-15(H_2O_2) presents an obvious weight loss at about 87 °C due to physisorbed water, while those due to the template are missing. The appearance of gentle weight loss above 150 °C might be mainly assigned to the condensation of surface hydroxyl group [25]. Similar phenomena have also been observed by Melián–Cabrera et al. on the study of detemplation of beta zeolite by Fe^{3+}–H_2O_2 solution [25]. As for the TGA of SBA-15(C), it shows a quite similar process (not shown here). It is important to note that the amount of physisorbed water in the SBA-15(H_2O_2) sample (ca. 13 wt%) is significantly larger than for the calcined SBA-15 material (ca. 5 wt%). This is an indirect evidence that porosity has been developed and water enters into the channels of SBA-15(H_2O_2). Mesoporosity formation was confirmed by N_2 adsorption–desorption measurements. The pore size distribution (Fig. 1B), calculated according to the BJH method from the adsorption branch of the isotherms, confirms the presence of mesoporosity in the Fe^{3+}–H_2O_2 treated material.

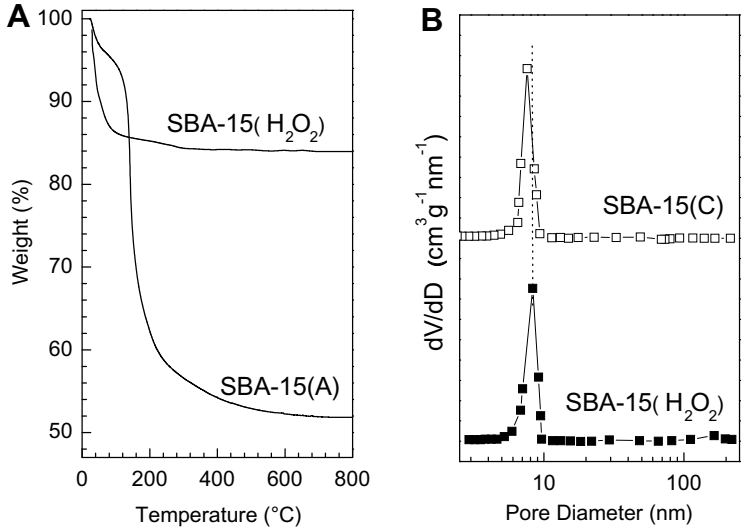

Fig. 1. (A) Thermogravimetric (TG) curves of SBA-15(A) and SBA-15(H_2O_2), (B) Pore distribution of SBA-15(H_2O_2) and SBA-15(C).

The absence of triblock copolymer template in the SBA-15(H_2O_2) material can be further confirmed by the infrared spectroscopic (IR) analysis (Fig. 2). The C–H stretching and C–H bending or deformation vibrations at around 2850–2900 and 1240–1500 cm^{-1} are clearly observed in the as-synthesized SBA-15(A). However, these characteristic bands are totally absent in SBA-15(H_2O_2). This indicates that the template is indeed removed by H_2O_2 treatment, which is in agreement with the TG analyses. In contrast to SBA-15(A), the typical bands due to siliceous material Si–O–Si, i.e. a main band at 1070 cm^{-1}, with a shoulder at 1200 cm^{-1}, due to asymmetric Si–O–Si stretching modes, as well as the corresponding symmetric stretch at 810 cm^{-1}, are observed for SBA-15(H_2O_2). More importantly, a significant modification in the narrow vibration band at 3740 cm^{-1} belonging to isolated terminal silanol groups (see inset to Fig. 2), indicative of the presence of enriched surface hydroxy species, is identified for SBA-15(H_2O_2) as compared with that for a SBA-15(C) material. It is also worthwhile to note that the spectrum in the hydroxyl region of the SBA-15(H_2O_2) sample display a broad absorption band between 3760 and 3300 cm^{-1} (centered at ca. 3660 cm^{-1}) due to OH-stretching vibrations of geminal and associated terminal silanol groups [28], giving further evidence the presence of a high abundance of silanol groups on the pore wall surface.

XRD patterns obtained for SBA-15(H_2O_2)-supported vanadia samples (V-loadings from 1.5 to 8.0 wt.%) are depicted in Fig. 3. For comparison purpose, the diffraction data recorded for SBA-15(C) is also included. All the materials show well-defined XRD patterns corresponding to typical SBA-15 structures, implying the overall mesoporous hexagonal structure after V incorporation is retained. A shift of the diffraction peaks to lower 2θ values relative to the SBA-15(C) material is identified for SBA-15(H_2O_2), possibly due to a less structural shrinkage during the low temperature template removal step. Additionally, a slight increase in the intensity of the d_{100} peak is identified in SBA-15(H_2O_2). The consequence of

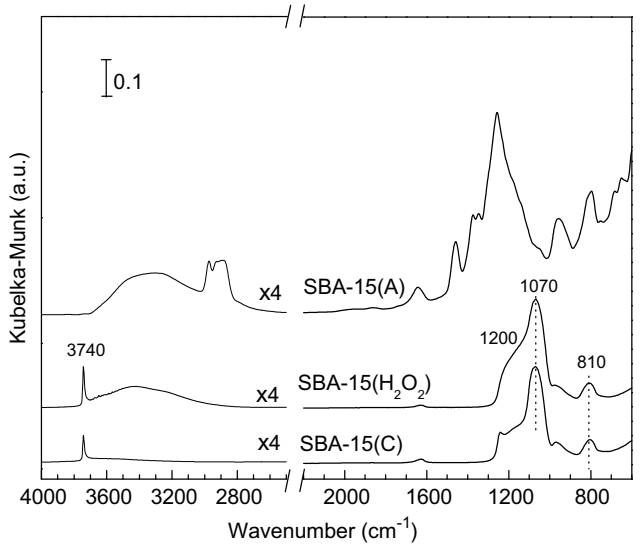

Fig. 2. DRIFT spectra of SBA-15(A), SBA-15(H_2O_2) and SBA-15(C).

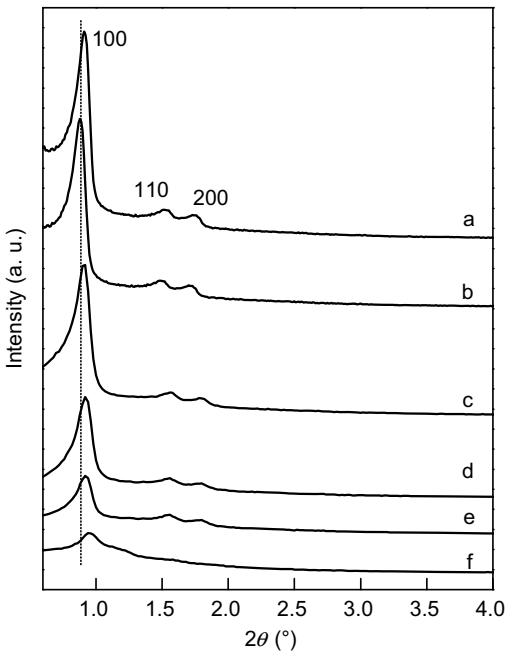

Fig. 3. Low-angle X-ray diffraction patterns of SBA-15-supported vanadia catalysts: (a) SBA-15(C); (b) SBA-15(H_2O_2); (c) 1.5V-SBA-15(H_2O_2); (d) 3.0V-SBA-15(H_2O_2); (e) 4.5V-SBA-15(H_2O_2); (f) 9.0V-SBA-15(H_2O_2).

such phenomena could be a well maintenance of the mesoporous SBA-15 structure as previously reported for zeolitic BEA system [25]. After vanadium incorporation, a continuous shift of the diffraction peaks to higher 2θ values is registered for the V-SBA-15(H_2O_2) samples. Moreover, it is seen that the intensity of the d_{100} peak is gradually attenuated with increasing V-loading in the XRD patterns of the samples. The reduction of the reflections in the higher loaded V-SBA-15(H_2O_2) samples might be caused by a degradation of the hexagonal arrangement of SBA-15 pores [26,29]. Nevertheless, based on the TEM analysis as shown in Fig. 4, it seems more likely due to a dilution of the silica matrix with increased incorporation of vanadia as a result of higher adsorption factor for X-rays than silicon [30].

The maintenance of ordered hexagonal arrangement of the SBA-15(H_2O_2) frameworks upon vanadium deposition is further supported by the N_2-adsorption data. Although the incorporation of vanadia into SBA-15 led to a continuous decrease of the specific surface area and the cumulative pore volume (Table 1), high surface areas (S_{BET}) and pore volumes as well as very narrow pore size distribution are observed in SBA-15-supported materials with V-loading up to 9.0 wt.%. The pore volume and the specific surface area of sample 9.0V-SBA-15(H_2O_2) is obviously larger than that of the calcined SBA-15(C) loaded vanadia sample, suggesting that new material shows many benefits such as larger surface areas and pore volume after vanadium incorporation. It is remarkable that a very high specific surface area and pore volume of about 464 $m^2\,g^{-1}$ and 0.5 $cm^3\,g^{-1}$ could be remained for 9.0V-SBA-15(H_2O_2), in contrast to an almost totally loss of the mesoporous structure previously reported for a 10V-M41S material [18]. Thus it can be concluded that well-organized mesoporous V-SBA-15(H_2O_2) catalysts with higher structure stability could be obtained at V-loadings as high as 9.0 wt% in the present study.

Fig. 5 shows the Raman spectra, recorded in the 200–1200 cm^{-1} range, of SBA-15 (H_2O_2)-supported vanadia catalysts dehydrated at 450 °C. For the V-SBA-15(H_2O_2) samples with V-content lower than 4.5 wt%, the Raman bands at 490, 605, 1034, 1074 cm^{-1} are observed. When vanadium content in the sample is 9.0 wt%, four additional bands at 283, 405, 690 and 991 cm^{-1} characteristic of crystalline V_2O_5 are detected. Band at 490 cm^{-1} is associated with the vibration of the siloxane rings of siliceous SBA-15(H_2O_2) [31]. The 1034 cm^{-1} band is attributed to the symmetric stretching mode of the V=O bond of the isolated tetrahedral VO_4 species [21,32,33]. The Raman band at 1074 cm^{-1} are characteristic of Si(–O–)$_2$ functionality [34], which has been assigned to perturbed silica vibrations that are indicative of the formation of V–O–Si bonds [35]. The absence of a typical band at ca. 991 cm^{-1} of V_2O_5 in Fig. 5a–c implies that no crystalline V_2O_5 is formed in V-SBA-15(H_2O_2) samples with V-content lower than 4.5 wt.%. All these results suggest that the vanadium species in V-SBA-15(H_2O_2) sam-

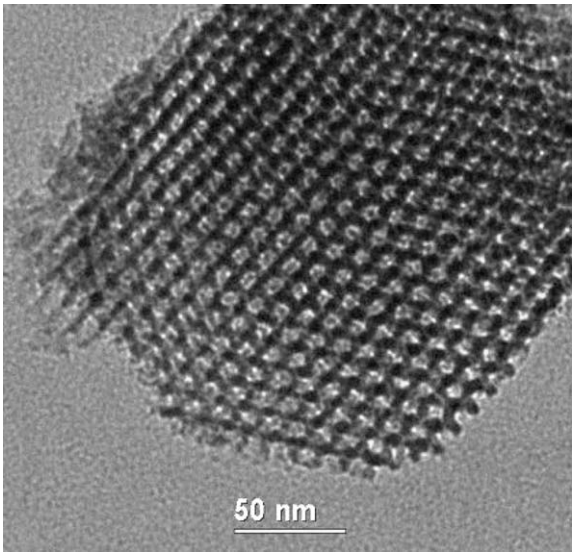

Fig. 4. TEM image of sample 9.0V-SBA-15(H_2O_2) after calcination.

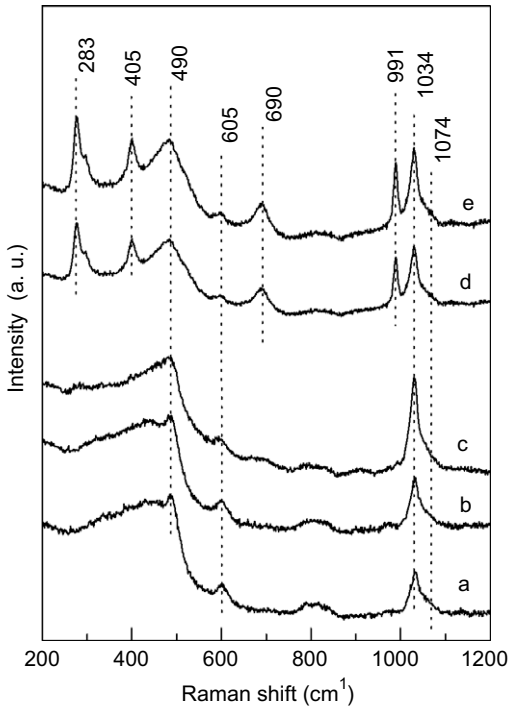

Fig. 5. Visible Raman spectra of SBA-15(H_2O_2) and SBA-15(C) supported vanadia catalysts after dehydration at 450 °C in air for 2 h: (a) 1.5V-SBA-15(H_2O_2); (b) 3.0V-SBA-15(H_2O_2); (c) 4.5V-SBA-15(H_2O_2); (d) 9.0V-SBA-15(H_2O_2); (e) 4.5V–SBA-15(C).

Table 1
Physico–chemical properties of the supported vanadia catalysts

Sample[a]	V-density (VO_x per nm^2)	S_{BET} ($m^2\,g^{-1}$)	D_{BJH}[b] (nm)	V_p ($cm^3\,g^{-1}$)	H_2-TPR T_M (°C)[c]
SBA-15(H_2O_2)	–	772	8.0	1.28	–
SBA-15(C)	–	695	7.6	1.23	–
1.5V-SBA-15(H_2O_2)	0.27	667	7.6	0.83	523
3.0V-SBA-15(H_2O_2)	0.59	603	7.4	0.75	524
4.5V-SBA-15(H_2O_2)	1.01	525	6.8	0.47	524
9.0V-SBA-15(H_2O_2)	2.29	464	5.6	0.50	546
4.5V-SBA-15(C)	1.18	451	6.1	0.40	545

[a] The actual V-contents measured by ICP-AES is the same with the nominal loading.
[b] The pore size distribution (PSD) determined based on the BJH method.
[c] Temperature of the maximum hydrogen consumption (T_M).

ples are isolated or, at least, highly dispersed on the surface of the SBA-15(H_2O_2) materials [21,35,36].

For a comparative purpose the Raman spectra of vanadia supported on SBA-15(C) is also depicted in Fig. 5. In contrast with sample 4.5V-SBA-15(H_2O_2) as shown in Fig. 4c, the band at 991 cm^{-1} can be easily observed in the Raman spectra of 4.5V-SBA-15(C) (Fig. 4e). According to a recent investigation by Iglesia et al. [37], the ratio of scattering cross-sections for bulk V_2O_5 and isolated tetrahedral VO_4 has been estimated to be 10. Using this ratio of Raman cross-sections and assuming that only V_2O_5 crystallites and isolated VO_4 species are present, the ratio of V_2O_5:VO_4 for the 8.0 wt% of V–MCF sample is estimated to be 0.05. The VO_x concentrations at which V_2O_5 is observed (>2.15 V nm^2, see Table 1) are well below those required for a monolayer of polymeric vanadia (~10 V nm^2), calculated on the basis of the literature value for the cross-sectional area of a $VO_{5/2}$ group of 0.103 nm^2 [38]. This indicates that the VO_x surface species tend to form larger clusters, when a certain VO_x concentration is reached.

Fig. 6 presents the H_2-TPR profile of SBA-15(H_2O_2)-supported vanadia catalysts from 200 to 700 °C. The catalysts studied show one (low or medium V-loadings) or two reduction bands (high V-loadings), which are apparently related to the V-species observed by Raman analysis. The catalysts with low and medium V-loadings (1.5–4.5 wt%) present one reduction band with reduction temperature maxima (T_M) at ca. 524 °C, that, in agreement with Raman results, should be determined by the reduction of isolated tetrahedral V^{5+} species. A similar band at 546 °C is also observed for high V-loading catalysts (9.0 wt% of V-atoms), although a second band in the 550–650 °C range is also detected. According to the literature and our previous results [22], this last band is very likely related to the presence of V_2O_5 crystallites and to the band at 991 cm^{-1} in Raman spectra observed in silica- or MCM-41 supported vanadia catalysts [18–20]. The high reduction temperature of crystalline V_2O_5 is due to the low accessibility of lattice vanadium atoms in the V_2O_5 bulk [39]. From the intensity of the reduction bands it can be concluded that the presence of V_2O_5 is more abundant than other samples in the catalyst with the highest metal loading (9.0V-SBA-15(H_2O_2)).

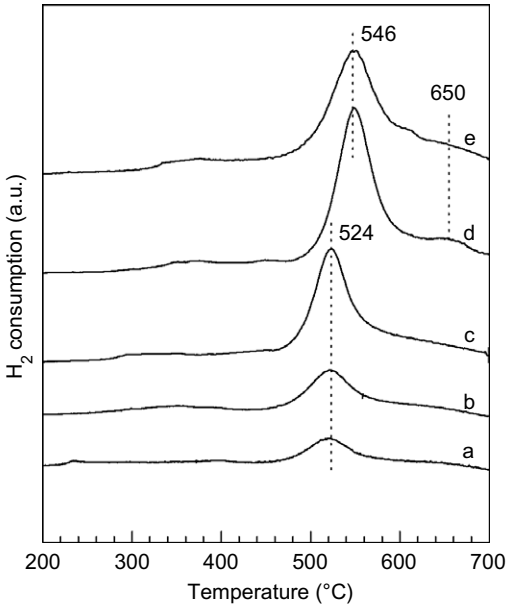

Fig. 6. H_2-TPR results of SBA-15-supported vanadium oxide catalysts: (a) 1.5V-SBA-15(H_2O_2); (b) 3.0V-SBA-15(H_2O_2); (c) 4.5V-SBA-15(H_2O_2); (d) 9.0V-SBA-15(H_2O_2); (e) 4.5V–SBA-15(C).

3.2. Catalytic results in the ODH of propane

Catalytic results with SBA-15(H_2O_2)-supported vanadia catalysts are shown in Table 2. Blank results show that negligible homogenous reaction could occur under the reaction conditions employed here. The vanadium-free support gives very poor catalytic activity being CO_x (CO and CO_2) practically the only reaction product detected. This low activity is consistent with the inferior activity of silica or other siliceous materials as reported in the literature [20–22], indicating that the presence of trace amount of Fe impurity has no essential influence on the catalytic behavior of the parent material for ODH of propane. The products on all the V-loaded catalysts are mainly C_3H_6 and CO_x, accompanied by small amounts of C_2H_4, CH_4 and oxygenates.

The results, reported in Table 2, point to a marked composition effect on the catalytic performance of the *n*V-SBA-15(H_2O_2) samples. Additionally, with a similar V-content, SBA-15(H_2O_2) is much superior to SBA-15(C) as a support. Higher dispersion and isolation of the active species of V present on the SBA-15(H_2O_2) surface can be attributed to the enhanced catalytic performance in the ODH of propane to propylene. The highest propylene yield of 25.3% is attained on the 4.5V-SBA-15(H_2O_2) catalyst, which results in a high space-time yield (STY_{C3H6}) of 3.42 kg propylene per kg cat^{-1} h^{-1} under reaction conditions. It should be pointed out that an industrially interesting STY_{C3H6} would be at least at 1 kg propylene per kg cat^{-1} h^{-1} [40]. In the present study, the STY_{C3H6} obtained with V-SBA-15(H_2O_2) catalysts is well above this value and marginally close to those with V–MCF catalysts most recently reported [22].

Fig. 7 shows the evolution of the catalytic activity and the turnover frequency (TOF, per atom of vanadium) with the vanadium loading for SBA-15(H_2O_2)-supported vanadia catalysts. Obviously,

Table 2
Oxidative dehydrogenation of propane on the supported vanadia catalysts at 600 °C[a]

Catalyst	χ (C_3H_8) (100%)	*S* (%)					*Y* (C_3H_6) (%)	*Y* (olefin[c]) (%)	STY (C_3H_6)[d] (kg kg cat^{-1} h^{-1})
		C_3H_6	C_2H_4	Oxygenates[b]	CO	CO_2			
SBA-15(C)	9.3	22.6	2.9	4.4	49.3	20.7	2.1	2.4	0.28
SBA-15(H_2O_2)	11.6	23.4	2.7	5.1	48.4	20.3	2.7	3.0	0.36
1.5V-SBA-15(H_2O_2)	27.1	63.0	7.0	4.2	12.2	2.8	17.1	19.0	2.30
3.0V-SBA-15(H_2O_2)	37.1	59.8	12.1	–	13.6	3.9	22.2	26.7	3.00
4.5V-SBA-15(H_2O_2)	44.2	57.2	17.9	–	15.6	3.3	25.3	33.2	3.42
9.0V-SBA-15(H_2O_2)	46.2	42.4	6.4	–	24.9	6.9	19.6	22.5	2.64
4.5V-SBA-15(C)	44.8	43.5	9.9	–	38.5	2.2	19.5	23.9	2.63

[a] Reaction conditions: W_{cat} = 25 mg; C_3H_8:O_2:N_2 = 1.0:1.0:4.0; GHSV = 43,200 L kg cat^{-1} h^{-1}.
[b] Partial oxygenated products, i.e. acrolein and trace amount of acetaldehyde.
[c] Light olefins, i.e. C_3H_6 and C_2H_4.
[d] Space-time yield of propylene.

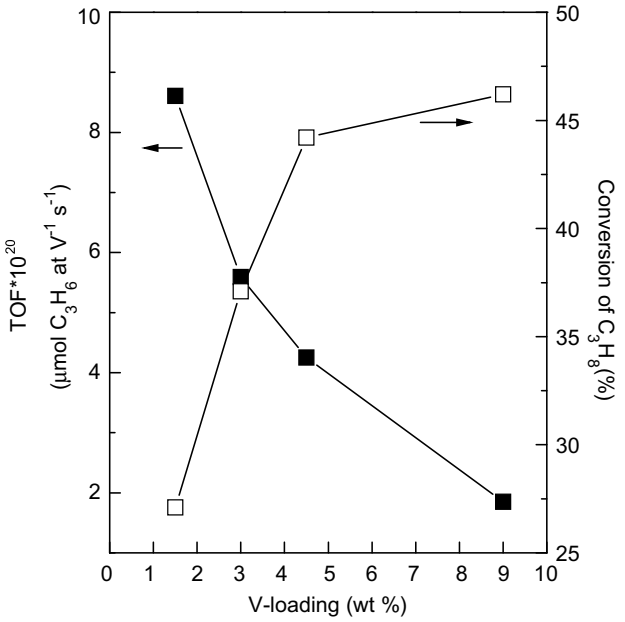

Fig. 7. Variation of the propane conversion and TOF with the V-loading of SBA-15(H_2O_2)-supported vanadia catalysts, reaction temperature = 600 °C.

an increase in the propane conversion and a decrease in the TOF could be observed. The drop in the activity per vanadium atom can be associated with the presence of vanadium atoms non-accessible to the propane reactant molecules. To gain further insight into the possible influence of the nature of the siliceous support on the catalytic behavior of V-catalysts, the variation of the selectivity's to propylene with the two 4.5V-loaded siliceous mesoporous catalysts at three different propane conversion levels is compared in Fig. 8. It is seen that the selectivity to propylene decreases with the propane conversion on both samples. At the same propane conversion levels, 4.5V-SBA-15(H_2O_2) demonstrates higher selectivity to propylene than 4.5V-SBA-15(C). However, at low alkane conversion (15%) the variation of selectivity with the two catalysts is very small (ca. 4–6%). This fact, together with previous

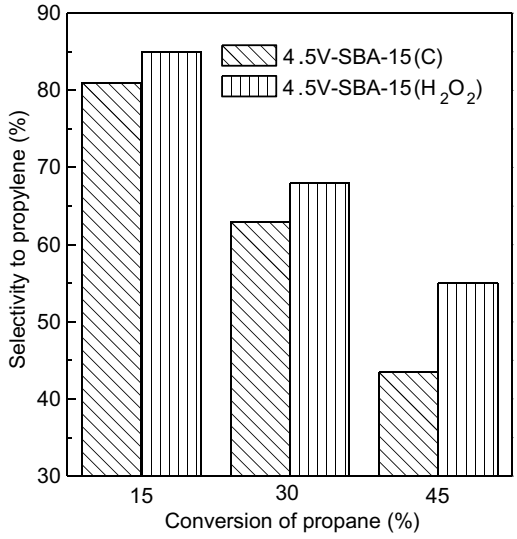

Fig. 8. Variation of the selectivity to propylene with the different propane conversion levels obtained during the oxidation of propane at 600 °C on 4.5V-SBA-15(H_2O_2) and 4.5V-SBA-15(C) catalysts.

reported activity data [20–22], confirms that to establish the real catalytic behavior of a catalyst the results at relatively high propane conversions must be studied [18], since the catalytic data obtained only at low conversions can lead to erroneous conclusions.

As it has been widely reported, the catalytic behavior of supported vanadium oxide catalysts in the selective oxidation of light alkanes depends strongly on the dispersion of vanadium loaded on the metal oxide supports [1,3]. Isolated tetrahedral vanadium oxide species containing terminal V=O groups below monolayer surface converge have been suggested as the active sites for the selective formation of propylene [18–22]. The dispersion of the supported vanadia layers on SiO_2; however, is generally less than 100% monolayer coverage because of the lower reactivity and greater acidic character of the silica surface hydroxyls [41]. Indeed, it is known that 100% dispersion of vanadia on conventional silica can only be achieved with vanadium loadings lower than 2.0 wt% [26]. Thus from the practical point of view, it is particular challenging to achieve a high dispersion of the VO_x species at vanadium loading as high as possible.

Using siliceous SBA-15 as support with a surface area higher than 700 $m^2\ g^{-1}$ good vanadium dispersions on the support can be achieved. In fact, a remarkable selectivity to propylene was obtained with medium vanadium loadings up to 2.8 wt% of V. This amount of vanadium oxide roughly equals what is required for monolayer formation (ca. 0.70 V nm^{-2}) over silica, which is far beyond what is needed for MCM-41 (ca. 2.4 wt%) and conventional silica [21]. More recently, we have further demonstrated that the use of mesoporous MCF silica as novel support can allow the generation of new efficient V-containing catalyst with much higher vanadium loadings up to 4.2 wt% (~V coverage of 1.08 V nm^2) [22]. It is important to note that, in this case, the amount of vanadia already far exceeds what is required for monolayer formation over silica supports. The excellent V-dispersion capability of MCF has been attributed to the presence of a high abundance of surface silanol groups thus can allow the favorable creation of a higher surface concentration of isolated VO_x species in the V–MCF system.

In the present investigation, the best performance for the ODH of propane was observed with the V-SBA-15(H_2O_2) catalyst containing 4.5 wt% V. Only isolated VO_x species were present in this catalyst, as evidenced by Raman spectroscopy. This is an advantage associated with the SBA-15(H_2O_2) material, which allows higher V-loading before bulk V_2O_5 begins to segregate. In contrast, when SBA-15(C) is used as a support, the amount of vanadia exceeds what is required for monolayer formation, leading to polymeric or V_2O_5 formation at V-loadings below those for the present V-SBA-15(H_2O_2) samples. This is likely due to the unique surface nature of the latter samples, which exhibited much higher surface Si–OH concentrations that is a prerequisite for isolated VO_x sites accommodation [22,42]. On the other hand, it is important to note that the scission of some Si–O–Si siloxane bridges during the preparation process also may have favored the formation of V–O–Si bonds and thus the generation of isolated VO_x species at concentrations greater than those usually obtained with SBA-15(C) silica.

Our findings in the present study confirm that the hydroxyl groups facilitates the preparation of new generation of V-containing mesoporous silica catalysts with enhanced content of dispersed VO_x species and helps prevent the formation of crystalline V_2O_5, especially in catalysts with high surface area and moderate V coverage (~1.01 V nm^{-2}). At this juncture, it is interesting to point out that the presence of acid sites, as silanol groups, at the surface of different vanadium containing catalysts has been reported to be active and selective to CO_x in the oxidation of propane [6,8]. However, in the present work the amount of surface OH groups in the support does not appear to play a negative role on the overall selectivity to propylene. This could be accounted for by the fact that the reactivity of vanadium sites is remarkably higher than that

of the unselective OH groups (see catalytic activity of SBA-15(H_2O_2) support Table 2).

4. Conclusion

This study demonstrates that H_2O_2-detemplated SBA-15 is new attractive support applicable for the fabrication of new promising V-containing mesoporous catalysts highly effective for the oxidative dehydrogenation of propane. The best catalyst achieved a yield to propylene of ca. 25%. In contrast to the SBA-15(C), the high abundance of silanol groups of the SBA-15(H_2O_2) allowed a very good dispersion of vanadium oxide on its surface leading to high productivities of propylene in the oxidative dehydrogenation of propane. The most selective vanadium sites for the ODH of propane resulted to be isolated tetrahedral V^{5+} species. An additional advantage of SBA-15(H_2O_2) as support vs. conventional calcination-derived SBA-15 is that the introduction of high vanadium loadings to siliceous SBA-15(H_2O_2) does not collapse its structure, leading to higher catalytic activity and selectivity to propylene.

Acknowledgments

This work was financially supported by the National Natural Science Foundation of China (20421303, 20473021, and 20633030), the National High Technology Research and Development Program of China (2066AA03Z336), the National Basic Research Program of China (2003CB615807), the Shanghai Science and Technology Committee (07QH14003) and Shanghai Education Committee (06SG03).

References

[1] F. Cavani, N. Ballarini, A. Cericola, Catal. Today 127 (2007) 113.
[2] A. Adamski, Z. Sojka, K. Dyrek, Langmuir 15 (1999) 5733.
[3] B. Frank, A. Dinse, O. Ovsitser, E.V. Kondratenko, R. Schomäcker, Appl. Catal. A 323 (2007) 66.
[4] K. Chen, A. Khodakov, J. Yang, A.T. Bell, E. Iglesia, J. Catal. 186 (1999) 325.
[5] E.V. Kondratenko, M. Cherian, M. Baerns, Catal. Today 112 (2006) 60.
[6] T. Blasco, J.M. López Nieto, Appl. Catal. A 157 (1997) 117.
[7] G. Martra, F. Arena, S. Coluccia, F. Frusteri, A. Parmaliana, Catal. Today 63 (2000) 197.
[8] A.A. Teixeira-Neto, L. Marchese, G. Landi, L. Lisi, H.O. Pastore, Catal. Today 133 (2008) 1.
[9] M. Chaar, D. Patel, M. Kung, H.H. Kung, J. Catal. 109 (1988) 463.
[10] A. Klisińska, K. Samson, I. Gressel, B. Grzybowska, Appl. Catal. A 309 (2006) 10.
[11] I. Rossetti, L. Fabbrini, N. Ballarini, C. Oliva, F. Cavani, A. Cericola, B. Bonelli, M. Piumetti, E. Garrone, H. Dyrbeck, E.A. Blekkan, L. Forni, J. Catal. 256 (2008) 45.
[12] N. Ballarini, F. Cavani, A. Cericola, Catal. Today 127 (2007) 113.
[13] X. Rozanska, E.V. Kondratenko, J. Sauer, J. Catal. 256 (2008) 84.
[14] S.A. Karakoulia, K.S. Triantafyllidis, A.A. Lemonidou, Micropor. Mesopor. Mater. 110 (2008) 157.
[15] M. Puglisi, F. Arena, F. Frusteri, V. Sokolovskii, A. Parmaliana, Catal. Lett. 41 (1996) 41.
[16] L. Owens, H.H. Kung, J. Catal. 144 (1993) 202.
[17] J. Le Bars, J.C. Vedrine, A. Auroux, S. Trautman, M. Baerns, Appl. Catal. A 88 (1992) 179.
[18] B. Solsona, J.M. Lopez Nieto, U. Diaíz, Miropor. Mesopor. Mater 94 (2006) 339.
[19] A. Khodakov, B. Olthof, A.T. Bell, E. Iglesia, J. Catal. 181 (1999) 205.
[20] Y. Wang, Q.H. Zhang, Y. Ohishi, T. Shishido, K. Takehira, Catal. Lett. 72 (2001) 215.
[21] Y.M. Liu, Y. Cao, N. Yi, W.L. Feng, W.L. Dai, S.R. Yan, H.Y. He, K.N. Fan, J. Catal. 224 (2004) 417.
[22] Y.M. Liu, W.L. Feng, T.C. Li, H.Y. He, W.L. Dai, W. Huang, Y. Cao, K.N. Fan, J. Catal. 239 (2006) 125.
[23] S. Meri, H. Selcuk, M. Gallo, V. Belgiorno, Desalination 173 (2005) 239.
[24] D.Y. Zhao, J.L. Feng, Q.S. Huo, N. Melosh, G.H. Fredrickson, B.F. Chmelka, G.D. Stucky, Science 279 (1998) 548.
[25] I. Meliań-Cabrera, F. Kapteijn, J.A. Moulijn, Chem. Commun. (2005) 2178.
[26] R. Zhou, Y. Cao, S.R. Yan, J.F. Deng, Y.Y. Liao, B.F. Hong, Catal. Lett. 75 (2001) 107.
[27] Y.M. Wang, Z.Y. Wu, L.Y. Shi, J.H. Zhu, Adv. Mater. 17 (2005) 323.
[28] H. Berndt, A. Martin, A. Brückner, E. Schreier, D. Müller, H. Kosslick, G.-U. Wolf, B. Lücke, J. Catal. 191 (2000) 384.
[29] B. Solsona, T. Blasco, J.M.L. Nieto, M.L. Peña, F. Rey, A. Vidal-Moya, J. Catal. 203 (2001) 443.
[30] L. Vradman, M.V. Landau, M. Herskowitz, V. Ezersky, M. Talianker, S. Nikitenko, Y. Koltypin, A. Gedanken, J. Catal. 213 (2003) 163.
[31] K.J. Chao, C.N. Wu, H. Chang, L.J. Lee, S.F. Hu, J. Phys. Chem. B 101 (1997) 6341.
[32] R. Rulkens, J.L. Male, K.W. Terry, B. Olthof, A. Khodakov, A.T. Bell, E. Iglesia, T.D. Tilley, Chem. Mater. 11 (1999) 2966.
[33] Z.H. Luan, P.A. Meloni, R.S. Czernuszewicz, L. Kevan, J. Phys. Chem. B 101 (1997) 9046.
[34] P. McMillan, Am. Mineral. 69 (1986) 622.
[35] X. Gao, S.R. Bare, B. Weckhuysen, I.E. Wachs, J. Phys. Chem. B 102 (1998) 10842.
[36] Y.M. Liu, Y. Cao, S.R. Yan, W.L. Dai, K.N. Fan, Catal. Lett. 88 (2003) 61.
[37] S. Xie, E. Iglesia, A.T. Bell, Langmuir 16 (2000) 7162.
[38] A.J. Van Hengstum, J.G. Van Ommen, H. Bosch, P.J. Gellings, Appl. Catal. 5 (1983) 207.
[39] F. Ying, J. Li, C.J. Huang, W.Z. Weng, H.L. Wan, Catal. Lett. 115 (2007) 137.
[40] J.B. Stelzer, J. Caro, M. Fait, Catal. Commun. 6 (2005) 1.
[41] A. Klińsinska, S. Loridant, B. Grzybowska, J. Stoch, I. Gressel, Appl. Catal. A 309 (2006) 17.
[42] W. Liu, S.Y. Lai, H. Dai, S. Wang, H. Sun, C.T. Au, Catal. Today 131 (2008) 450.